Data-Driven Approaches to Predict the Stability Metrics of Catalytic Nanoparticles

Asmee M. Prabhu[1] and Tej S. Choksi[1*]

1. School of Chemical and Biomedical Engineering, 62 Nanyang Drive, Nanyang Technological University, Singapore, 637459.

Corresponding author: tej.choksi@ntu.edu.sg

Abstract

A prevailing challenge in computational catalyst design is to discover nanostructures which are thermodynamically stable and synthesizable in practice. Important metrics for the stability of nanostructures include the chemical potential of supported nanoparticles, cohesive energies of nanoparticles, surface and adhesion energies of crystal planes that bound the nanoparticle, and segregation energies in bimetallic nanoparticles. *Ab initio* methods can accurately calculate these metrics but are computationally intensive due to the large configurational space that these nanostructures span. Moreover, sub-nm nanoparticles are structurally flexibility under reaction conditions. Hence, physics-based & machine-learning-derived data-driven approaches are becoming prevalent to determine the stability of nanostructures. In this review we discuss the recent advances in data-driven methods to predict stability metrics of nanoparticles.

Highlights

- Overview of data driven methods to compute nanoparticle stability metrics.
- Stability metrics include chemical potentials and cohesive energies of nanoparticles, surface energies of crystal planes, adhesion energies of supported nanoparticles, and segregation energies in bimetallic nanoparticles.
- Physics based and machine learning approaches are employed to predict the stability metrics of both atomically dispersed clusters and large nanoparticles.

Key words: Nanoparticles, Catalyst stability, Machine learning, Data science, Bimetallic Alloys, Single site catalysts

1. Introduction

Reactivity, selectivity & stability represent the holy trinity in heterogeneous catalysis but are rarely studied concurrently. While the computational design of reactive and selective nanoparticle catalysts is well-established [1,2], considerations for nanoparticle stability in high-throughput-screening have emerged more recently [3-13]. An enduring challenge in *in silico* catalyst design is to design nanoparticles that are: (1) thermodynamically stable under reaction conditions and (2) synthesizable in practice. The first step in determining the potential synthesizability of nanoparticles is to evaluate their thermodynamic stability. For sub-nm particles, low energy metastable structures are accessible under temperatures typical to thermal catalysis [11,14]. Therefore, while determining thermodynamic stability, it is necessary to focus on both global minima and low energy isomers of nanoparticles. Catalytic nanoparticles span a wide range of sizes, shapes, compositions, and chemical ordering. While first-principles methods like density functional theory (DFT) can accurately evaluate the thermodynamic stability of these nanostructures; these methods remain computationally intensive. To reduce computational cost, data-driven models for evaluating nanoparticle stability metrics have emerged.

This focused review covers data-driven models for determining four metrics of nanoparticle stability, namely: (1) the chemical potential of supported nanoparticles [3,15,16], (2) cohesive energies of nanoparticles [7,10,13,17-20], (3) surface and adhesion energies of crystal planes which bound the nanoparticle [3,4,8,15,21,22], and (4) segregation energies in bimetallic nanoparticles [5,6,10]. The cohesive energy is the energy gained in forming a nanoparticle from metal atoms in the gas phase, thus indicating nanoparticle stability. Surface and adhesion energies represent the energies required to cleave crystal planes from bulk structures and to separate a metal nanoparticle from its support respectively. Segregation energies represent energy changes due to re-ordering of atoms in a bimetallic nanoparticle. We discuss these stability metrics for both sub-nm clusters and larger nanoparticles (diameters > 2 nm). Data-driven methods for determining nanoparticle stability will open avenues for operando computational design [23]; wherein rates and selectivity are evaluated on catalyst structures that exist under reaction conditions.

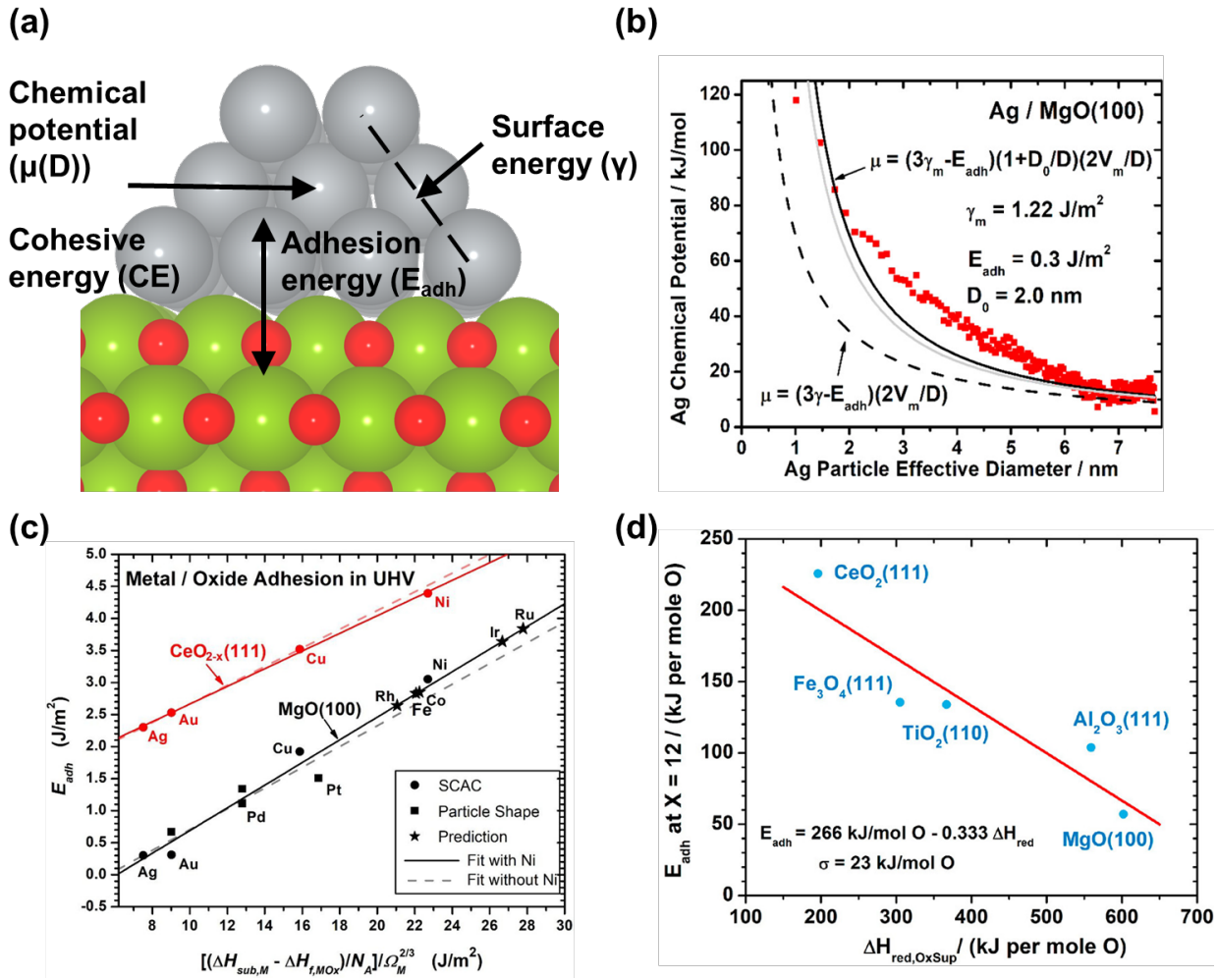

Figure 1: (a) Ag nanoparticle supported on MgO (100). Stability metrics like chemical potential, cohesive energy, adhesion energy, and surface energy are marked. Ag, Mg, and O are depicted in grey, green, and red respectively. **(b)** Experimentally measured chemical potential of Ag supported on MgO (red points). The solid black line indicates estimates from **equation 1.** Reprinted with permission from Ref [16]. Copyright (2021) American Chemical Society. **(c)** Adhesion energies of different metals on a given support are directly proportional to the metal oxophilicity (**equation 2**). Reprinted with permission from Ref [3]. Copyright (2017) American Chemical Society. **(d)** Adhesion energies at a given oxophilicity for different supports are inversely proportional to the reducibility of the support (**equation 3**). Reprinted with permission from Ref [3]. Copyright (2017) American Chemical Society.

2. Predicting the chemical potential of supported nanoparticles from experiments

The chemical potential of nanoparticles has emerged as a descriptor for both their reactivity towards small molecules and for sintering [16]. Experiments [3,15,16] and computational reports [22,24] indicate that metal nanoparticles with higher (lower) chemical potential bind adsorbates

strongly (weakly). Such stability-reactivity relations have also been experimentally observed on perovskites [25]. Campbell et al. [3] expressed the chemical potential of a supported metal nanoparticle using **equation 1.**

$$\mu(D) = \left[(3\gamma_M - E_{adh})\left(1 + \frac{D_0}{D}\right)\right]\frac{2V_M}{D} + (\Delta H_{sub} - \Delta H_{sub^*}) \quad (1)$$

For a given nanoparticle diameter (D), the chemical potential (μ) is computed using the surface energy (γ_M), metal-support adhesion energy (E_{adh}), molar volume (V_M), and a correction factor ($D_0 \approx 1.5$ nm) for size effects [26,27] prevalent in nanoparticles smaller than ~ 4 nm. For metals like Ni, an additional term ($\Delta H_{sub} - \Delta H_{sub^*}$) accounts for the difference in the sublimation energy between the bulk phase of the nanoparticle (e.g., hcp) and the most stable bulk phase of the metal (e.g., fcc) [16]. Since γ_M, V_M, and ΔH_{sub} are available in databases, **equation 1** yields the chemical potential of arbitrary supported metal nanoparticles provided E_{adh} and, if applicable, ΔH_{sub^*} are known. Campbell et al. [3] predicted the E_{adh} using simple correlations involving physicochemical properties of supported metal nanoparticles as inputs **(Figure 1).** For a given support (e.g., MgO) and different transition metals, they observed a linear correlation (**equation 2**) between the experimentally measured E_{adh} and the metal oxophilicity (X). The metal oxophilicity per area is the heat of formation of the metal's most stable oxide from metal and oxygen atoms in the gas phase. This oxophilicity (X) is computed as the difference between the metal sublimation energy ($\Delta H_{sub,m}$) and the heat of formation of its most stable oxide ($\Delta H_{f,MOx}$).

$$E_{adh} = slope \cdot X + intercept, \quad X = \frac{[\Delta H_{sub,m} - \Delta H_{f,MOx}]}{V_M^{\frac{2}{3}}} \quad (2)$$

$$E_{adh,\ X=12} = -0.333\ \Delta H_{red,OxSup} + 266 \quad (3)$$

For a given metal oxophilicity (e.g., X = 12 in **equation 3**), the E_{adh} across different oxide supports correlate linearly with the reducibility of the support (**equation 3**). The reducibility is determined from the enthalpy of reduction of the oxide support to its next lowest oxidation state ($\Delta H_{red,OxSup}$). The correlation in **equation 3** has a negative slope, indicating that weakly adsorbed oxygen atoms in reducible oxides form stronger bonds with the metal atoms of the nanoparticle. This explanation

is congruent with the bond order conservation principle [28]. **Equations 1, 2, and 3** form a general model to estimate the chemical potential of supported metal nanoparticles having arbitrary sizes. This model predicts chemical potentials with errors of 10-20 % [3].

The experimentally derived correlations in **equations 2 and 3** have guided first-principles-based statistical learning approaches [4,29-32] which estimated the adhesion energies of transition metals on oxide supports. Statistical models [4,29-32] based on these experiments [3,15,16] uncovered similar features driving metal/support adhesion; namely, the oxophilicity of the metal, the reducibility of the support, and the density of oxygen atoms. Hence, the experimentally measured chemical potential of metal atoms can calibrate the statistical learning models, thereby increasing their accuracy.

3. Computing the cohesive energies of metal nanoparticles

Cohesive energies of nanoparticles have a similar interpretation as the chemical potential of nanoparticles discussed in **section 2.** The magnitude of the cohesive energy reflects the overall stability of a nanoparticle, referenced to metal atoms in the gas phase. More stable nanoparticles have higher magnitudes of cohesive energies. Structure-energy relationships to estimate cohesive energies of nanoparticles have been derived using physics-based [7,10,13,17,18,20,33] and machine-learning-approaches [19,34]. From the wide range of approaches already established, we highlight two methods to predict cohesive energies.

Yan et al. [13] developed the bond centric model which predicts the cohesive energy (CE) of bimetallic nanoparticles in terms of the bulk cohesive energy (CE_{Bulk}) and coordination numbers (CN_i or CN_j) of each metal, i and j **(equation 4).** This model is derived from the square-root bond-cutting model [13]. The bond centric model splits the cohesive energy into half bond energy contributions for each metal, i and j. These contributions are fused together using metal dependent weights (γ_i, γ_j). **Equation 4** can determine the cohesive energies of bimetallic nanoparticles having different morphologies, compositions & chemical ordering. The weights, γ, are computed using bond dissociation energies of bimetallic clusters derived from either experiments or theory [13]. We note that the bond centric model captures the DFT energetics accurately for CuAg bimetallic systems **(Figure 2a).**

$$CE = \frac{\sum_1^m \gamma_i \times \frac{CE_{Bulk-i}}{CN_i}\sqrt{\frac{CN_i}{12}} + \gamma_j \times \frac{CE_{Bulk-j}}{CN_j}\sqrt{\frac{CN_j}{12}}}{n} \quad (4)$$

Since **equation 4** is analytical, it was recast within a mixed-integer linear program to identify optimally stable nanoparticles [35]. For bimetallic clusters, the optimization problem was decomposed into a mixed-integer linear program which optimized the chemical ordering, and a simulated annealing framework which modified cluster shapes [36]. These two steps were combined within an iterative co-optimization process (**Figure 2b**) and used to quantify how the size and composition of AgCu, AuAg and CuAu nanoclusters influences their overall cohesion [36]. Maximizing the stability of nanoparticles by modifying their composition can also be achieved using a genetic algorithm [17].

The alloy stability model proposed by Abild-Pedersen and co-workers [7,10,20,37,38] partitions energies of metal atoms into contributions arising from individual metal-metal bonds ($\alpha_{\substack{z=site\ identity \\ i=coordination\ number}}$). This model explicitly considers the coordination numbers of nearest neighbours with mean-field treatments for compositional variations. Streibel et al. [20] incorporated strain effects within this approach. The energies of metal atoms, in turn, yield the stability of atomic sites, cohesive energies, and surface energies. Since these coordination-based models were derived from extended surfaces and bulk structures, they have limited accuracy for disordered structures and for particles below ~2 nm [26,27]. For nanoparticles below 2 nm, the machine learning approach proposed by Lamoureux et al. [7] outperforms the linear form of the alloy stability model. A genetic algorithm was used to identify the five most-important features for describing metal-metal interactions in the machine learning model. These features include readily available properties like interatomic distances, coordination numbers, atomic numbers, etc. **Figure 2c** illustrates how features of the machine learning model evolve with increasing nanoparticle size. As the nanoparticle size increases, interatomic distances and bond angles diminish in importance while the importance of chemical composition and coordination numbers is enhanced.

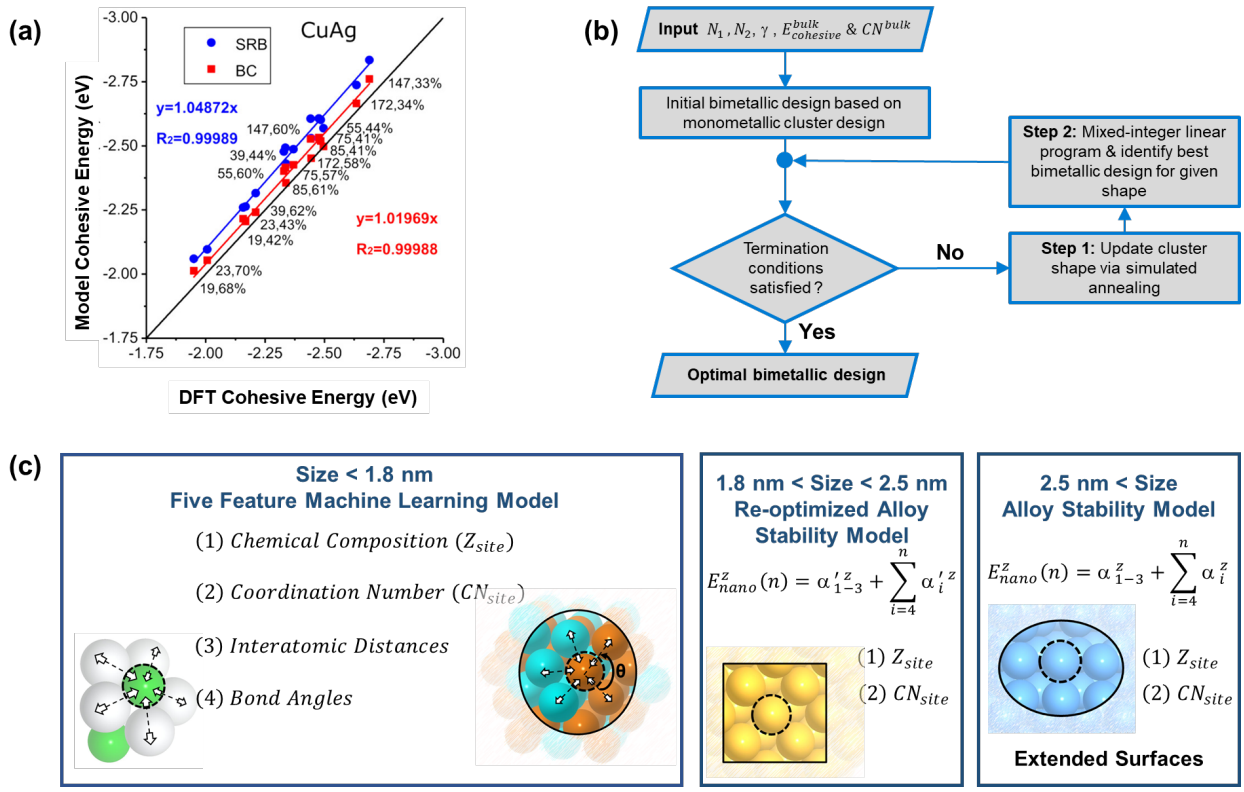

Figure 2: (a) Parity plot between model predicted (Bond Centric and Square-root Bond Cutting models) and DFT-derived cohesive energies for CuAg nanoparticles. Labels indicate total number of atoms in the nanoparticle and the percentage of Ag in the CuAg nanoalloys. Reprinted with permission from Ref. [13]. Copyright 2018 American Chemical Society. **(b)** Two-step optimization strategy for identifying bimetallic nanoclusters with high cohesive energies. Reproduced from Ref. [36] with permission from the Royal Society of Chemistry. **(c)** Evolution of best-performing features with increasing particle size. In the sub-nanometer to nanometer size regime, machine learning models are needed to accurately determine stability metrics. These models use features like the site identity (Z_{site}), site coordination number (CN_{site}), interatomic distances, bond angles, etc. As the nanoparticle size increases, structural features diminish in importance with the site identity and the site coordination number remaining as the two most important features. Reproduced from Ref. [7] with permission from the Royal Society of Chemistry.

Although predicting nanoparticle stability in vacuum is well-established, further progress in determining nanoparticle stability under reaction conditions is necessary, to bridge the materials gap in catalysis. Cohesive energy models integrated with optimization algorithms [35,36] enable the inverse design of nanoparticles; wherein the chemical structure is optimized such that a pre-specified cohesive energy is obtained.

4. Estimating surface energies, adhesion energies, and segregation energies

The nanoparticles discussed in earlier sections can be deconstructed into crystal planes which bound their surfaces. The stability of these crystal planes is reflected by their surface energy. The surface energy is a fundamental property that influences nanoparticle equilibrium morphology [1], surface stability against reconstruction [39] and segregation [6]. Ma et al. established a method based on chemical intuition to predict surface energies using the concept of generalized atomic valence [21]. Surface energies are represented by a simple geometric descriptor - the degree of surface undercoordination. The degree of surface undercoordination quantifies the disorder of intermolecular bonds based on the coordination environment of surface atoms. Their model predicted surface energies of body-centred cubic (BCC), face-centred cubic (FCC), and hexagonal close-packed (HCP) transition metal surfaces with a root mean standard error of 0.087 J/m^2 (**Figure 3a**). This model was extended to other high-index non-symmetrical facets and used to estimate the equilibrium crystal morphology for group VIII transition metals. In contrast to monometallic structures, the cleavage of intermetallic bulk alloys along crystal planes yield asymmetric slabs. The surface energy of these slabs is termed as the cleavage energy. Palizhati et al. [8] formulated an *ab initio* workflow to predict cleavage energies of intermetallic alloys using high-throughput DFT and a crystal graph convolutional neural network. They predicted the cleavage energy of 3033 intermetallic alloys with combinations of 36 elements and 47 space groups with a mean absolute test error of 0.0071 eV/A^2.

Metal nanoparticles are anchored on supports to prevent sintering and exploit electronic metal-support interactions for chemical reactions [40,41]. In such cases the adhesion energy between the metal and support determines the particle shape & energetics. Dietze et al. [4] proposed an intuitive model (**equation 5**) to predict adhesion energies (E_{adh}) for a given metal−oxide system using two descriptors: (1) the adsorption energy of atomic oxygen on clean metal surfaces ($E_{adsorption}(O)$) & (2) the concentration of interfacial oxygen atoms making interface metal-oxygen bonds (c_O). These descriptors are consistent with experimental models [3,15,16] discussed in **section 2**. **Figure 3(b)** shows the parity plot depicting model predicted and DFT calculated adhesion energies of metal films on oxide supports.

$$E_{adh} \approx \left(E_{adsorption}(O)\alpha + \beta\right)c_o \quad (5)$$

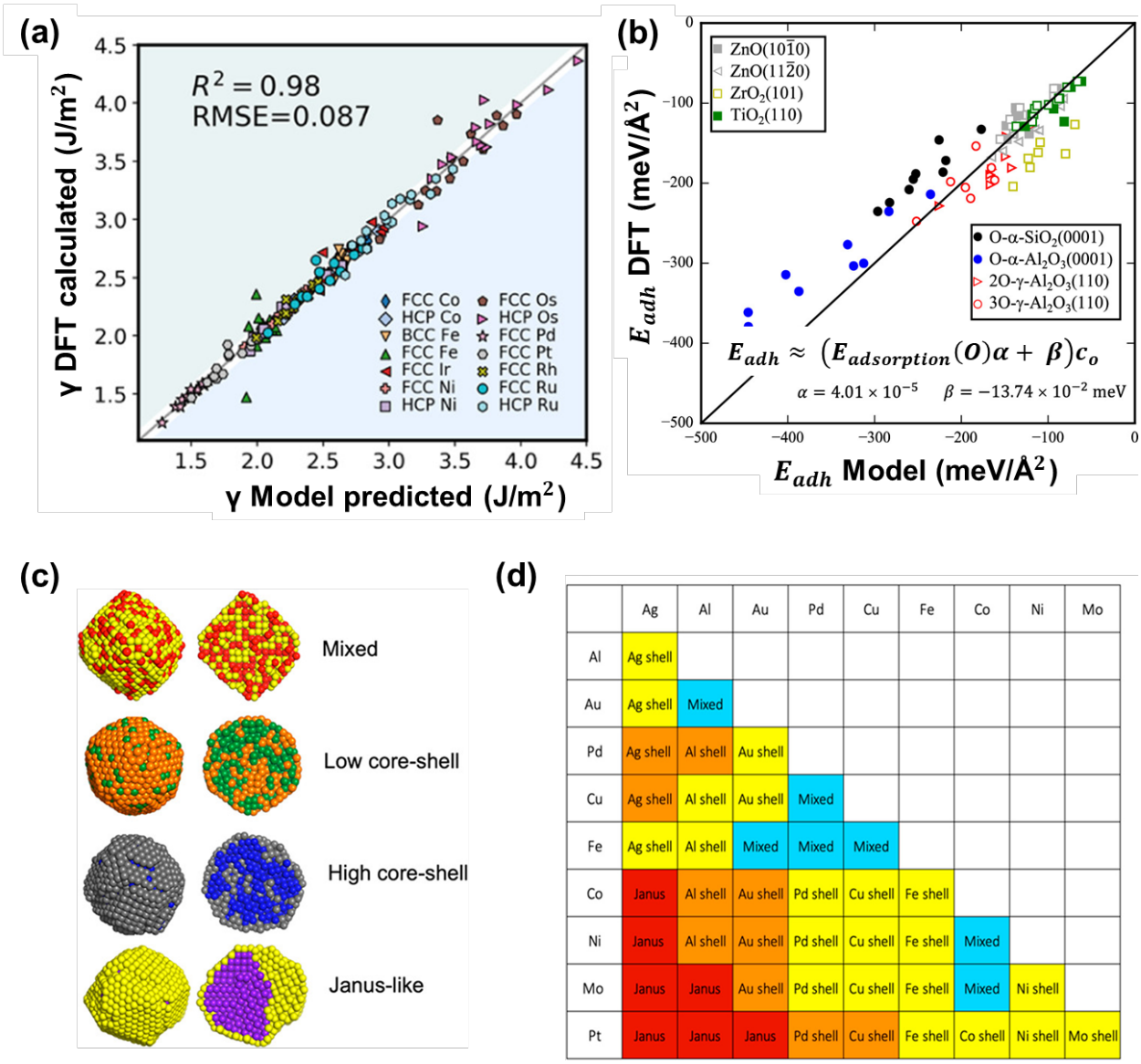

	Ag	Al	Au	Pd	Cu	Fe	Co	Ni	Mo
Al	Ag shell								
Au	Ag shell	Mixed							
Pd	Ag shell	Al shell	Au shell						
Cu	Ag shell	Al shell	Au shell	Mixed					
Fe	Ag shell	Al shell	Mixed	Mixed	Mixed				
Co	Janus	Al shell	Au shell	Pd shell	Cu shell	Fe shell			
Ni	Janus	Al shell	Au shell	Pd shell	Cu shell	Fe shell	Mixed		
Mo	Janus	Janus	Au shell	Pd shell	Cu shell	Fe shell	Mixed	Ni shell	
Pt	Janus	Janus	Janus	Pd shell	Cu shell	Fe shell	Co shell	Ni shell	Mo shell

Figure 3: (a) Comparing DFT-derived and model-predicted surface energies (γ) using the concept of generalized atomic valence for relaxed surfaces. Reprinted with permission from Ref. [21]. Copyright (2020) American Chemical Society. **(b)** Parity plot depicting predicted and calculated adhesion energies of metal films on oxide supports using the adsorption energy of oxygen on the metal as a descriptor. Reprinted with permission from Ref. [4]. Copyright (2019) American Chemical Society. **(c)** Four morphologies of bimetallic nanoparticles based on segregation patterns: mixed, low-level core−shell, high level core−shell, and Janus-like core-shell structures. The cross-sectional view is on the right side. Reprinted with permission from Ref. [5]. Copyright (2021) The Authors. Published by American Chemical Society. **(d)** Segregation preferences for bimetallic nanoparticles classified according to the four morphologies shown in (c). Reprinted with permission from Ref. [5]. Copyright (2021) The Authors. Published by American Chemical Society.

For bimetallic nanoparticles, the energy needed to alter the relative ordering of the two elements is called as the segregation energy. Segregation energies of bimetallic nanoparticles dictate their preference to form mixed, low level core−shell, high level core−shell or Janus-like core structures [5] (structures in **Figure 3c**) and thus play a crucial role in nanoparticle synthesis and applications [42]. Using molecular dynamics and Monte Carlo simulations, Eom et al. [5] determined trends in how core−shell preferences change with metal composition for 45 bimetallic systems (**Figure 3d**). Using principal component analysis and linear discriminant analysis they found that both the Wigner−Seitz radius difference and cohesive energy difference together dictate the degree of segregation in an "additive" manner. Each element was scored with a higher score provided for a large cohesive energy and a smaller radius. The elements are arranged in the order of increasing score (left to right/ top to bottom in **Figure 3d**) to form a lower triangular matrix. Mixed structures lie along the diagonal & the highly segregated Janus-like structures lie near the right-angled vertex. Segregation energies can be predicted using adsorption energies of molecular fragments. Liu et al. [43] observed that the segregation energies in bimetallic systems scale linearly with the difference between the adsorption energy of CO_2 hydrogenation intermediates on the two pristine metal surfaces that compose the bimetallic structure. Farsi et al. [6] developed a statistical model which predicts the segregation energy of transition metal dopants. This model uses as inputs the d-band width (W^B), d-band filling of the dopant (N_B), coordination number in the surface (Z_S) and in the bulk (Z_B), elastic energy release $\left(\left[\left(\frac{r_B}{r_A}\right)^3 - 1\right]^2 r_A^3\right)$, and the surface energy ($E_{Surface}^{Metal}$) difference of the host and the dopant. **Equation 6** can distinguish segregation patterns in different stepped and terraced surfaces (including (100), (111), (110) & (210)).

$$E_{Segregation}^{B\to A} = \beta_0 + \beta_1 W^B + \beta_2 N_B + \beta_3 \left(E_{Surface}^{B} - E_{Surface}^{A}\right) + \beta_4 \left[\left(\frac{r_B}{r_A}\right)^3 - 1\right]^2 r_A^3 + \beta_5 \left[1 - \left(\frac{Z_b}{Z_s}\right)^{\frac{1}{2}}\right] \quad (6)$$

Accelerated schemes to determine surface energies [8,21,38], adhesion energies [4], and segregation energies [6,10,17,36] can generate equilibrium morphologies of bimetallic nanoparticles on-the-fly. Computational models employing such nanoparticle morphologies for

catalysis studies are a step-change from ubiquitous low-miller-index crystal planes. For nanoparticles in the sub-nm size regime, special approaches are needed. These approaches are discussed in **section 5.**

5. Evaluating the stability of atomically dispersed catalysts

Atomically dispersed catalysts maximize precious metal loading while unlocking unique catalytic properties [44]. Predicting the thermodynamic stability of atomically dispersed catalysts is essential to both establish the driving force for sintering [30,31], and to find metastable states beyond the global minimum which contribute to reaction rates [11,14]. We discuss data-driven approaches to estimate stability metrics of single atom alloys, single atoms adsorbed on supports, and of supported sub-nm clusters.

Rao et al. [9] determined whether promoters added to a transition metal host preferentially exist as single atom alloys, dimers, single atoms in the subsurface, or as adatoms. Their best performing model (errors ~ 0.2 eV) integrates a physics-based bond counting approach with a machine learned error correction term. This hybrid approach enables accurate transferability to new structures without changing the input vector. Han et al. [45] predicted the stability of single atom alloys in the presence of adsorbed hydrogen using compressed sensing. This method generates new descriptors by combining low-cost primary features (e.g., cohesive energy, d-band centre, ionization potential etc.) with mathematical operators (e.g., +, -, ·, and ⁄). It would be exciting to unleash such techniques originally formulated for extended surfaces, onto nanoparticles, to uncover if quantum- and finite-size effects stabilize different compositions of single atom alloys.

The stability of single site catalysts dispersed on oxide supports is governed by adsorption energies [29-32] and diffusion barriers [46] of metal atoms. O'Connor et al. [31] forecasted the adsorption energies of single metal atoms on oxides using compressed sensing. Compressed sensing operations indicate that the adsorption energies of metal atoms depends on the metal oxophilicity (enthalpy of oxide formation), and the oxide reducibility (oxygen vacancy formation energy in the support). These features are consistent with experiments [3,15,16] (**Figure 1**) and linear models [4]. Descriptors for metal-support interaction established for single atoms on one support (MgO) were transferable to chemically similar supports (CaO, BaO, ZnO), demonstrating the robustness of this method [30]. Data-driven approaches also generate intuitive, physically interpretable

models. Su et al. [46] used feature selection methods and genetic programming to build a scaling law for the diffusion barriers of d-block single metal atoms on diverse supports (**equation 7**). This empirical relationship expresses diffusion barriers (E_a) using both the metal adsorption energy (E_{bind}) and the metal cohesive energy (E_C) as descriptors.

$$E_a = 0.636\frac{E_{bind}^2}{E_C} - 0.203 \quad (7)$$

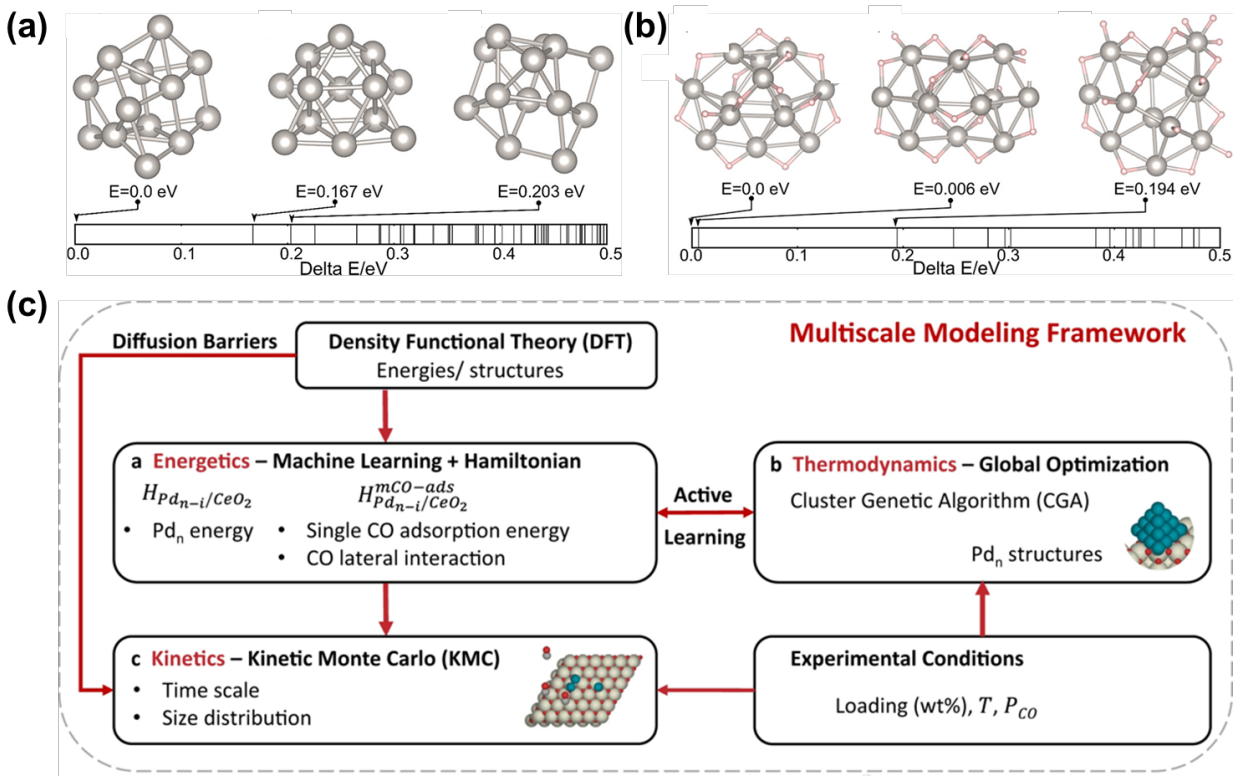

Figure 4: (a)-(b) Low energy metastable structures for bare Pt_{13} and H* covered Pt_{13}. Pt and H atoms are in grey and pink respectively. The three lowest energy structures are shown. Reprinted with permission from Ref. [11]. Copyright (2018) American Chemical Society. **(c)** Multiscale model which unites different Hamiltonians for determining the stability of CO* covered sub-nm Pt particles. The energy outputs from the Hamiltonians and DFT-calculated diffusion barriers are inputs to kinetic monte carlo simulations. Reprinted with permission from Ref. [12]. Copyright (2021) The Authors. Published by Springer Nature.

Single atom catalysts can sinter under reaction conditions forming sub-nm clusters [12]. Under the high temperatures prevalent in catalysis, isomers of sub-nm clusters interconvert across several low energy metastable structures [11,14]. Such low energy metastable clusters often dominate the

overall rate [11]. Data-driven approaches are necessary to exhaustively sample these metastable structures and to efficiently evaluate their stability. Sun et al. [11] modified a genetic algorithm, which typically identifies global minima, to specifically find low energy metastable structures. This genetic algorithm is powered by a high dimensional neural network potential [11,47]. This potential computes the total energies of the clusters using symmetry functions based on the local chemical environment. Sun et al. [11] deployed these sampling and energy prediction methods to identify low energy metastable Pt structures in vacuum (**Figure 4a**) and in the presence of hydrogen (**Figure 4b**). These metastable structures displayed higher rates for hydrogen evolution and methane activation. While the thermodynamic stability of sub-nm clusters is important, their morphological changes are kinetically controlled. Wang et al. [12] formulated a multiscale model (**Figure 4c**) to investigate the dynamics of Pd nanoclusters supported on CeO_2. Their approach integrates two cluster expansion Hamiltonians which determine the energies of bare Pd clusters and CO* covered clusters respectively. Sub-nm clusters are sampled using a genetic algorithm and the cluster expansion is trained using active learning, thus reducing computational cost. The diffusion barriers for Pd atoms and clusters are computed using density functional theory. The Hamiltonian models and diffusion barriers are inserted into kinetic Monte Carlo simulations, which determine the cluster dynamics. This multiscale workflow reveals that in CO environments, single atoms sinter rapidly forming flat Pd clusters which are kinetically trapped.

To effectively study the cluster dynamics of sub-nm catalytic nanoparticles, it is necessary to consider thermodynamic stability beyond the global minimum [11,12,34]. Data-driven approaches are vitally important in these tasks because they can (1) predict cluster stability on-the-fly [7,11,14,34], (2) efficiently sample metastable sub-nm clusters [11,34], and (3) uncover new structure-function relationships [30,31,45,46].

6. Outlook

Data-driven methods have enabled us to predict stability metrics of nanoparticles [3-5,7-11,13,20,30,34,36,38] with computational efficiencies on-par with evaluating descriptors for catalytic reactivity [28,48,49]. While these models predict internal energy changes with near-DFT accuracy, further developments are needed for estimating the entropy of nanoparticles. Can we build semi-empirical models to evaluate the entropy of the collective dynamics of metal atoms

[50] without needing molecular dynamics? These contributions to entropy are important for structurally flexible nanoparticles below ~ 2 nm diameters and for nanoparticles at elevated temperatures. Integrating on-the-fly determinations for stability and reactivity will enable inverse design through catalytic-property → structure connections. Including thermodynamic (meta)stability as constraints in inverse design [51,52] will engender realistic outputs of nanoparticle structures for a pre-specified catalytic property. We note that synthesizability metrics for nanomaterials may not always depend on thermodynamic (meta)stability [53]. Shifting from nanoparticle (meta)stability to nanoparticle synthesizability will require new descriptors discovered through the unity of data-driven methods for (meta)stability, controlled nanoparticle synthesis, and operando characterization.

7. Author Contributions

Asmee M. Prabhu: Investigation, Writing – Original Draft, Writing – Review & Editing, Visualization. **Tej S. Choksi:** Conceptualization, Investigation, Writing – Original Draft, Writing – Review & Editing, Visualization, Supervision.

8. Acknowledgements

This work is supported by the Ministry of Education Academic Research Fund Tier 1: RS 04/19 and RG5/21 and the start-up grant from the College of Engineering, Nanyang Technological University (NTU), Singapore. A.M.P. gratefully acknowledges Nanyang Technological University for a research scholarship.

9. References

1. Barmparis GD, Lodziana Z, Lopez N, Remediakis IN: **Nanoparticle shapes by using Wulff constructions and first-principles calculations**. *Beilstein Journal of Nanotechnology* 2015, **6**:361-368.
2. Gauthier JA, Stenlid JH, Abild-Pedersen F, Head-Gordon M, Bell AT: **The Role of Roughening to Enhance Selectivity to C2+ Products during CO2 Electroreduction on Copper**. *ACS Energy Letters* 2021, **6**:3252-3260.
3. Campbell CT, Mao Z: **Chemical Potential of Metal Atoms in Supported Nanoparticles: Dependence upon Particle Size and Support**. *ACS Catalysis* 2017, **7**:8460-8466.
4. Dietze EM, Plessow PN: **Predicting the Strength of Metal–Support Interaction with Computational Descriptors for Adhesion Energies**. *The Journal of Physical Chemistry C* 2019, **123**:20443-20450.

•• Proposed a linear model to predict adhesion energies of metal films on oxide supports using two descriptors: the binding energy of oxygen on the metal surfaces and the concentration of interfacial oxygen atoms.

5. Eom N, Messing ME, Johansson J, Deppert K: **General Trends in Core–Shell Preferences for Bimetallic Nanoparticles**. *ACS Nano* 2021, **15**:8883-8895.

•• Practical guides for determining core-shell preference and the degree of segregation in bimetallic nanoparticles.

6. Farsi L, Deskins NA: **First principles analysis of surface dependent segregation in bimetallic alloys**. *Physical Chemistry Chemical Physics* 2019, **21**:23626-23637.
7. Lamoureux PS, Choksi TS, Streibel V, Abild-Pedersen F: **Combining artificial intelligence and physics-based modeling to directly assess atomic site stabilities: from sub-nanometer clusters to extended surfaces**. *Physical Chemistry Chemical Physics* 2021, **23**:22022-22034.

•• Integrated physics-based and machine-learning methods to predict the stability of nanoparticles ranging from sub-nm clusters, 1-2 nm diameter, to extended surfaces. Identified how the features governing metal nanoparticle stability evolve with increasing nanoparticle size.

8. Palizhati A, Zhong W, Tran K, Back S, Ulissi ZW: **Toward Predicting Intermetallics Surface Properties with High-Throughput DFT and Convolutional Neural Networks**. *Journal of Chemical Information and Modeling* 2019, **59**:4742-4749.
9. Rao KK, Do QK, Pham K, Maiti D, Grabow LC: **Extendable Machine Learning Model for the Stability of Single Atom Alloys**. *Topics in Catalysis* 2020, **63**:728-741.

•• Established a hybrid physics-based and machine learning method to predict the stability of single atom alloys, surface dimers, subsurface alloys, and adatoms for d-block transition metals.

10. Roling LT, Choksi TS, Abild-Pedersen F: **A coordination-based model for transition metal alloy nanoparticles**. *Nanoscale* 2019, **11**:4438-4452.
11. Sun G, Sautet P: **Metastable Structures in Cluster Catalysis from First-Principles: Structural Ensemble in Reaction Conditions and Metastability Triggered Reactivity**. *Journal of the American Chemical Society* 2018, **140**:2812-2820.

•• Demonstrated that metastable nanoclusters can contribute significantly to reaction rates. Developed a neural network potential and a modified genetic algorithm to identify such metastable clusters on bare- and adsorbate-covered nanoparticles.

12. Wang Y, Kalscheur J, Su Y-Q, Hensen EJM, Vlachos DG: **Real-time dynamics and structures of supported subnanometer catalysts via multiscale simulations**. *Nature Communications* 2021, **12**:5430.

•• Multi-scale model to understand the dynamics of supported nanoclusters under reaction conditions. Elucidated that kinetically trapped clusters are dominant. Showed that while considerations for thermodynamic (meta)stability are useful, they may not accurately represent nanocluster morphologies in reaction conditions.

13. Yan Z, Taylor MG, Mascareno A, Mpourmpakis G: **Size-, Shape-, and Composition-Dependent Model for Metal Nanoparticle Stability Prediction**. *Nano Letters* 2018, **18**:2696-2704.
14. Zhang Z, Zandkarimi B, Alexandrova AN: **Ensembles of Metastable States Govern Heterogeneous Catalysis on Dynamic Interfaces**. *Accounts of Chemical Research* 2020, **53**:447-458.
15. Hemmingson SL, Campbell CT: **Trends in Adhesion Energies of Metal Nanoparticles on Oxide Surfaces: Understanding Support Effects in Catalysis and Nanotechnology**. *ACS Nano* 2017, **11**:1196-1203.
16. Mao Z, Campbell CT: **Predicting a Key Catalyst-Performance Descriptor for Supported Metal Nanoparticles: Metal Chemical Potential**. *ACS Catalysis* 2021, **11**:8284-8291.

    •• Introduced a predictive model for the chemical potential of supported nanoparticles having arbitrary sizes. This model was derived using adsorption calorimetry. Important experimental study to benchmark computational models for metal-support interactions.

17. Dean J, Cowan MJ, Estes J, Ramadan M, Mpourmpakis G: **Rapid Prediction of Bimetallic Mixing Behavior at the Nanoscale**. *ACS Nano* 2020, **14**:8171-8180.
18. Dietze EM, Plessow PN, Studt F: **Modeling the Size Dependency of the Stability of Metal Nanoparticles**. *The Journal of Physical Chemistry C* 2019, **123**:25464-25469.
19. Jinnouchi R, Asahi R: **Predicting Catalytic Activity of Nanoparticles by a DFT-Aided Machine-Learning Algorithm**. *The Journal of Physical Chemistry Letters* 2017, **8**:4279-4283.
20. Streibel V, Choksi TS, Abild-Pedersen F: **Predicting metal–metal interactions. I. The influence of strain on nanoparticle and metal adlayer stabilities**. *The Journal of Chemical Physics* 2020, **152**:094701.
21. Ma H, Jiao Y, Guo W, Liu X, Li Y, Wen X-D: **Predicting Crystal Morphology Using a Geometric Descriptor: A Comparative Study of Elemental Crystals with High-Throughput DFT Calculations**. *The Journal of Physical Chemistry C* 2020, **124**:15920-15927.

    •• Proposed the concept of generalized atomic valence which is based on the degree of surface undercoordination. Used this descriptor to predict surface energies and estimate crystal morphologies for group VIII transition metals.

22. Roling LT, Abild-Pedersen F: **Structure-Sensitive Scaling Relations: Adsorption Energies from Surface Site Stability**. *ChemCatChem* 2018, **10**:1643-1650.
23. Grajciar L, Heard CJ, Bondarenko AA, Polynski MV, Meeprasert J, Pidko EA, Nachtigall P: **Towards operando computational modeling in heterogeneous catalysis**. *Chemical Society Reviews* 2018, **47**:8307-8348.

24. Choksi TS, Roling LT, Streibel V, Abild-Pedersen F: **Predicting Adsorption Properties of Catalytic Descriptors on Bimetallic Nanoalloys with Site-Specific Precision**. *The Journal of Physical Chemistry Letters* 2019, **10**:1852-1859.
25. Samira S, Gu X-K, Nikolla E: **Design Strategies for Efficient Nonstoichiometric Mixed Metal Oxide Electrocatalysts: Correlating Measurable Oxide Properties to Electrocatalytic Performance**. *ACS Catalysis* 2019, **9**:10575-10586.
26. Kleis J, Greeley J, Romero NA, Morozov VA, Falsig H, Larsen AH, Lu J, Mortensen JJ, Dułak M, Thygesen KS, et al.: **Finite Size Effects in Chemical Bonding: From Small Clusters to Solids**. *Catalysis Letters* 2011, **141**:1067-1071.
27. Li L, Larsen AH, Romero NA, Morozov VA, Glinsvad C, Abild-Pedersen F, Greeley J, Jacobsen KW, Nørskov JK: **Investigation of Catalytic Finite-Size-Effects of Platinum Metal Clusters**. *The Journal of Physical Chemistry Letters* 2013, **4**:222-226.
28. Greeley J: **Theoretical Heterogeneous Catalysis: Scaling Relationships and Computational Catalyst Design**. *Annual Review of Chemical and Biomolecular Engineering* 2016, **7**:605-635.
29. Iyemperumal SK, Pham TD, Bauer J, Deskins NA: **Quantifying Support Interactions and Reactivity Trends of Single Metal Atom Catalysts over TiO2**. *The Journal of Physical Chemistry C* 2018, **122**:25274-25289.
30. Liu C-Y, Zhang S, Martinez D, Li M, Senftle TP: **Using statistical learning to predict interactions between single metal atoms and modified MgO(100) supports**. *npj Computational Materials* 2020, **6**:102.

    •• Using statistical learning, created an interpretable model for estimating the binding energies of metal atoms on oxide supports. Demonstrated the generality of their model beyond MgO (training set for feature identification) to chemically similar oxides.

31. O'Connor NJ, Jonayat ASM, Janik MJ, Senftle TP: **Interaction trends between single metal atoms and oxide supports identified with density functional theory and statistical learning**. *Nature Catalysis* 2018, **1**:531-539.
32. Tan K, Dixit M, Dean J, Mpourmpakis G: **Predicting Metal–Support Interactions in Oxide-Supported Single-Atom Catalysts**. *Industrial & Engineering Chemistry Research* 2019, **58**:20236-20246.
33. Kozlov SM, Kovács G, Ferrando R, Neyman KM: **How to determine accurate chemical ordering in several nanometer large bimetallic crystallites from electronic structure calculations**. *Chemical Science* 2015, **6**:3868-3880.
34. Wang Y, Su Y-Q, Hensen EJM, Vlachos DG: **Finite-Temperature Structures of Supported Subnanometer Catalysts Inferred via Statistical Learning and Genetic Algorithm-Based Optimization**. *ACS Nano* 2020, **14**:13995-14007.
35. Isenberg NM, Taylor MG, Yan Z, Hanselman CL, Mpourmpakis G, Gounaris CE: **Identification of optimally stable nanocluster geometries via mathematical optimization and density-functional theory**. *Molecular Systems Design & Engineering* 2020, **5**:232-244.
36. Yin X, Isenberg NM, Hanselman CL, Dean JR, Mpourmpakis G, Gounaris CE: **Designing stable bimetallic nanoclusters via an iterative two-step optimization approach**. *Molecular Systems Design & Engineering* 2021, **6**:545-557.

•• Introduced a two-step optimisation framework to find optimally stable bimetallic nanoparticles. This framework integrates a mixed integer linear program for optimizing the chemical ordering, and a simulated annealing algorithm to sample structural space.

37. Choksi TS, Streibel V, Abild-Pedersen F: **Predicting metal–metal interactions. II. Accelerating generalized schemes through physical insights**. *The Journal of Chemical Physics* 2020, **152**:094702.
38. Roling LT, Li L, Abild-Pedersen F: **Configurational Energies of Nanoparticles Based on Metal–Metal Coordination**. *The Journal of Physical Chemistry C* 2017, **121**:23002-23010.
39. Warburton RE, Iddir H, Curtiss LA, Greeley J: **Thermodynamic Stability of Low- and High-Index Spinel LiMn2O4 Surface Terminations**. *ACS Applied Materials & Interfaces* 2016, **8**:11108-11121.
40. Nie L, Mei D, Xiong H, Peng B, Ren Z, Hernandez Xavier Isidro P, DeLaRiva A, Wang M, Engelhard Mark H, Kovarik L, et al.: **Activation of surface lattice oxygen in single-atom Pt/CeO2 for low-temperature CO oxidation**. *Science* 2017, **358**:1419-1423.
41. Whittaker T, Kumar KBS, Peterson C, Pollock MN, Grabow LC, Chandler BD: **H2 Oxidation over Supported Au Nanoparticle Catalysts: Evidence for Heterolytic H2 Activation at the Metal–Support Interface**. *Journal of the American Chemical Society* 2018, **140**:16469-16487.
42. Boes JR, Gumuslu G, Miller JB, Gellman AJ, Kitchin JR: **Estimating Bulk-Composition-Dependent H2 Adsorption Energies on CuxPd1–x Alloy (111) Surfaces**. *ACS Catalysis* 2015, **5**:1020-1026.
43. Liu S, Zhao Z-J, Yang C, Zha S, Neyman KM, Studt F, Gong J: **Adsorption Preference Determines Segregation Direction: A Shortcut to More Realistic Surface Models of Alloy Catalysts**. *ACS Catalysis* 2019, **9**:5011-5018.
44. Kaiser SK, Chen Z, Faust Akl D, Mitchell S, Pérez-Ramírez J: **Single-Atom Catalysts across the Periodic Table**. *Chemical Reviews* 2020, **120**:11703-11809.
45. Han Z-K, Sarker D, Ouyang R, Mazheika A, Gao Y, Levchenko SV: **Single-atom alloy catalysts designed by first-principles calculations and artificial intelligence**. *Nature Communications* 2021, **12**:1833.
46. Su Y-Q, Zhang L, Wang Y, Liu J-X, Muravev V, Alexopoulos K, Filot IAW, Vlachos DG, Hensen EJM: **Stability of heterogeneous single-atom catalysts: a scaling law mapping thermodynamics to kinetics**. *npj Computational Materials* 2020, **6**:144.
47. Sun G, Sautet P: **Toward Fast and Reliable Potential Energy Surfaces for Metallic Pt Clusters by Hierarchical Delta Neural Networks**. *Journal of Chemical Theory and Computation* 2019, **15**:5614-5627.
48. Montemore MM, Nwaokorie CF, Kayode GO: **General screening of surface alloys for catalysis**. *Catalysis Science & Technology* 2020, **10**:4467-4476.
49. Wang S-H, Pillai HS, Wang S, Achenie LEK, Xin H: **Infusing theory into deep learning for interpretable reactivity prediction**. *Nature Communications* 2021, **12**:5288.
50. Collinge G, Yuk SF, Nguyen M-T, Lee M-S, Glezakou V-A, Rousseau R: **Effect of Collective Dynamics and Anharmonicity on Entropy in Heterogenous Catalysis: Building the Case for Advanced Molecular Simulations**. *ACS Catalysis* 2020, **10**:9236-9260.

51. Ren Z, Noh J, Tian S, Oviedo F, Xing G, Liang Q, Aberle A, Liu Y, Li Q, Jayavelu S, et al.: **Inverse design of crystals using generalized invertible crystallographic representation**. *arXiv* 2020:2005.07609v07602.
52. Freeze JG, Kelly HR, Batista VS: **Search for Catalysts by Inverse Design: Artificial Intelligence, Mountain Climbers, and Alchemists**. *Chemical Reviews* 2019, **119**:6595-6612.
53. Jang J, Gu GH, Noh J, Kim J, Jung Y: **Structure-Based Synthesizability Prediction of Crystals Using Partially Supervised Learning**. *Journal of the American Chemical Society* 2020, **142**:18836-18843.